

# Synthesis, Characterization and Dissolution Performance of Cocrystal of Cinnamic Acid with Nicotinamide: Experimental and Computation Investigation

*by* Perpustakaan IIK Bhakti Wiyata

---

**Submission date:** 02-May-2026 08:41AM (UTC+0700)

**Submission ID:** 2501079557

**File name:** 5\_Publish\_RJPT\_papa\_-\_Iqbal\_Aljabir\_Pujiono.pdf (791.59K)

**Word count:** 8018

**Character count:** 43062

**RESEARCH ARTICLE**

**Synthesis, Characterization and Dissolution Performance of Cocystal of Cinnamic Acid with Nicotinamide: Experimental and Computation Investigation**

Fery Eko Pujiono<sup>1,2\*</sup>, I Setyawan<sup>3</sup>, Juni Ekowati<sup>3</sup>, Tri Ana Mulyati<sup>2</sup>

<sup>1</sup>Doctoral of Pharmacy, Faculty of Pharmacy, Airlangga University, Indonesia.

<sup>2</sup>Department of Pharmacy, Faculty of Pharmacy, Institut Ilmu Kesehatan Bhakti Wiyata, Indonesia.

<sup>3</sup>Department of Pharmaceutical Sciences, Faculty of Pharmacy, Airlangga University, Indonesia.

\*Corresponding Author E-mail: [ferypujiono@gmail.com](mailto:ferypujiono@gmail.com)


**ABSTRACT:**

Cinnamic acid cocystals have been synthesized with nicotinamide cofomers using the solvent evaporation method to produce white crystals. Characterization results with DSC show that cinnamic acid cocystals have different endothermic peaks of 110°C, cinnamic acid (136°C), and individual nicotinamide (127°C). PXRD results where cinnamic acid cocystals have different diffractogram patterns with individual cinnamic acid, namely diffractogram peaks at 6.7°, 13.4°, and 20.2°. The FTIR characterization results also indicate that cinnamic acid cocystals exhibit distinct FTIR spectra. Specifically, there is an absence of twin peaks in the wave number range of 3400-3000 cm<sup>-1</sup> corresponding to the -NH group, and absorption peaks resembling fusion appear at wave numbers around 1600 cm<sup>-1</sup> and 1500 cm<sup>-1</sup>, corresponding to -C=O and -C=C alkene groups. Additionally, SEM analysis reveals that while cinnamic acid has an irregular plate-like shape, the formed cocystals exhibit a smooth surface morphology and an irregular block-like shape. Furthermore, the solubility test demonstrates that the solubility of cinnamic acid increases from 0.57 g/100 ml to 1.09 g/100 ml after cocrystallization, indicating a 48% proportional enhancement in Dissolution Efficiency (DE) from 80.104% to 96.021%. The bond formation in the cocystal is a hydrogen bond, as indicated by the isosurface map and the RDG Scatter Plot. This bond occurs between the carboxylic group of cinnamic acid and the amide group of nicotinamide in the C=O<sub>C</sub>...N<sub>H</sub>-N synthon, as well as between the hydroxide group of cinnamic acid and the carboxylic group of nicotinamide in the O-H<sub>C</sub>...N<sub>O</sub>=C synthon. The hydrogen bond is represented by a blue spike at sign(λ<sub>2</sub>)ρ around -0.04 a.u.

**KEYWORDS:** Cocystals, Cinnamic acid, Nicotinamide, Dissolution, QTAIM.

**INTRODUCTION:**

Cinnamic acid is a secondary metabolite compound that is widely found in typical Indonesian plants such as frankincense sap (*Styrax Benzoin*)<sup>1</sup> and Laja Gowah (*Alpinia malaccensis* (Burm.f.))<sup>2,3</sup>. Cynamic acid is found in nature generally in a transform derived from the conversion of phenylalanine through the deamination reaction of the phenylalanine ammonium lyase enzyme on the shikimate pathway<sup>4</sup>. Sinamic acid has many biological activities as antimicrobial<sup>5</sup>, antifungal<sup>6</sup>, antioxidant<sup>7</sup>, and antidiabetic<sup>8</sup>. In addition to its many biological activities, cinnamic acid also has low toxicity<sup>9</sup>. However, cinnamic acid has a significant limitation in being developed as a candidate for new drug compounds: its low water solubility of 0.5 mg/L<sup>8</sup>. This makes it necessary to improve the water solubility value of the cinnamic acid.

Received on 19.09.2024    Revised on 13.01.2025  
Accepted on 18.03.2025    Published on 02.08.2025  
Available online from August 08, 2025  
*Research J. Pharmacy and Technology*, 2025;18(8):3929-3938.  
DOI: 10.52711/0974-360X.2025.00565  
RJPT All right reserved  
This work is licensed under a Creative Commons Attribution-NonCommercial-ShareAlike 4.0 International License. 

Their lipophilicity and intermolecular bonds generally influence the solubility of active pharmaceutical ingredients<sup>10</sup>. Efforts made to increase solubility due to high lipophilicity properties are solvency, micelle formation, and complexation, whilst, for compounds like cinnamic acid, whose viscosity problems are caused by strong intermolecular forces in the crystal lattice, the technique that can be used is the solid state technique<sup>11</sup>. Solid-state techniques can be carried out in several ways, such as forming salts, polymorphs, hydrates, solvates, and cocrystals<sup>12</sup>. A potential solid-state technique to be developed is cocrystallization. Cocrystals have advantages over salts (only for ionic molecules) because they can be used for ionic and non-ionic molecules; compared to salts, hydrates, and solvents, the structure of cocrystals can be modified without changing their pharmacological properties, and when compared to polymorphs, cocrystals have higher stability<sup>13,14</sup>. Cocrystal is a crystal engineering technique between Pharmaceutical Active Ingredients (BAF) and former through intermolecular bonds such as van der Waals,  $\pi$ - $\pi$ , and hydrogen interactions<sup>15-17</sup>.

Research on cocrystal to improve drug solubility has been widely conducted. Fael's<sup>18</sup> research on synthesizing 32 floxacin cocrystals with resorcinol conformers showed that the solubility of cocrystals was ten times greater than that of norfloxacin. Duan's research<sup>19</sup> also showed that palbociclib cocrystals with resorcinol cofomers showed thirteen times greater solubility than palbociclib. The research of Sabouri and Shayanfar<sup>20</sup> synthesizing carbamazepine cocrystals with succinic acid cofomers showed a ten-fold increase in solubility compared to carbamazepine. On the other hand, cinnamic acid has been used to manufacture cocrystals. However, it is still a cofomer as researchers Hiendrawan et al.<sup>21</sup> showed that itraconazole cocrystals with cinnamic acid cofomers have the highest solubility when compared to cofomers of suheic acid, sebacic acid, benzamide, and 1-hydro-2-naphthoic acid.

Currently, cocrystal research is being conducted by combining experimental and computational results to confirm the structure and intermolecular bonds in cocrystals<sup>22,23</sup>. One of the computational methods currently used in cocrystals is Quantum Theory Atoms in Molecules (QTAIM) of Bader<sup>24-27</sup>. QTAIM allows for quantitative analysis of bond strength by identifying Bond Critical Points (BCPs), which are points in space where electron density is at a maximum along the bond path between two atoms. This helps in understanding the strength and nature of intermolecular interactions, including hydrogen and halogen bonds<sup>28,29</sup>. Furthermore, QTAIM provides an analysis of electron density topology, which assists in identifying atomic basins and their properties. This topological approach allows for a detailed understanding of how atoms interact within

molecules or cocrystals, including the identification of hydrogen bond donors and acceptors<sup>26,30,31</sup>.

The Huang et al.<sup>28</sup> QTAIM study has been utilized in a systematic investigation of cocrystals, including sulfonamides such as sulfaguanidine. The analysis involves Hirshfeld surface, molecular electrostatic potential surface (MEPS), and QTAIM, providing a comprehensive understanding of hydrogen bond interactions in co-crystals. This aligns with Yadav et al.'s<sup>32</sup> research, which combines spectroscopy and quantum chemistry studies on the hydrochlorothiazide-nicotinamide cocrystal to confirm intermolecular hydrogen bonding that enhances the pharmacological properties of the cocrystal. Based on this background, this study combines experimental and computational results of cinnamic acid and nicotinamide cocrystals synthesized using the slow solvent evaporation method. The resulting cocrystals are further characterized by DSC, PXRD, ATR-FTIR, SEM, and computational analysis using QTAIM to determine the strength and nature of intermolecular bonding responsible for cocrystal formation. Additionally, in this study, solubility and dissolution rate analyses are conducted to assess pharmacological property enhancements.

## MATERIALS AND METHODS:

### Materials:

Trans-sinnamic acid (CA) ( $\geq 99\%$ ), Nicotinamide (NIC) ( $\geq 98\%$ ), and acetonitrile ( $\geq 99\%$ ) were purchased from Sigma-Aldrich.

### Cocrystalline CA-NIC synthesis:

The cocrystallization in this study uses a slow solvent evaporation method<sup>32</sup>. First, 0.2mmol of cinnamic acid is added with 10ml of acetonitrile dissolved in a stirring hot plate for 20 minutes. On the other hand, 0.2mmol of nicotinamide is added, and 10ml of acetonitrile is dissolved in a stirring hotplate for 20minutes. Next, a solution of cinnamic acid and nicotinamide is mixed on a stirring hot plate for 2hours. The solution was aged in a desiccator for five days to obtain white cinnamic acid and nicotinamide cocrystals (CA CC).

### Differential Scanning Calorimetry (DSC) Analysis:

DSC analysis uses a Mettler Toledo instrument to analyze CA, NIC, Physical Mixture of cinnamic acid and nicotinamide (CA PM), and CA CC. The instrument is calibrated by Indium for temperature and heat flow accuracy. Measurements were carried out in the temperature range of 30°C - 300°C with a heating rate of 10°C/min.

### Powder X-ray Diffraction (PXRD) Analysis:

PXRD analysis uses the PANalytic X'Pert PRO X-ray powder diffractometer to scan CA, NIC, CA PM, and CA CC. West Sumatra X-Raay is Cu-K $\alpha$  with a

wavelength of 1.540598 Å. The divergence and scattering slit were set to 1°, and receiving slit was set to 12.75mm. PXRD is performed by adjusting the voltage and current at 40kV and 30mA, respectively. The sample was placed in a quartz glass sample slide plane with an etched square and measured. Angular range (2θ) is 5.0084°-59.98614° at step times 10.1500 s and step size 0.0170°.

#### Attenuated Total Reflectance-Fourier Transform Infrared (ATR-FTIR) Analysis:

ATR-FTIR analysis uses Shimadzu IR-Prestige-21 with a horizontal Golden-Gate MKII single reflection ATR system equipped with ZnSe lenses to analyze CA, NIC, CA PM, and CA CC. The cocrystals' FT-IR spectra were collected in the range from 400 to 4000  $\text{cm}^{-1}$ .

#### Scanning Electron Microscopy (SEM) Analysis:

Morphological analysis of CA and CA CC using SEM Hitachi FLEXSEM 100. A 10mg sample is placed in a sample holder and coated with gold aluminum with a thickness of 10nm. The sample was then observed at a range of 500-5000 x with a voltage set at 20.0 kV.

#### Solubility Test:

The solubility test is conducted in distilled water using the shaking flask method. 25mg of CA, CA PM, and CA CC samples are dissolved in 25ml of phosphate buffer media (pH = 6.6) and stirred on a hot plate for 5 hours at 25±0.5°C. The subsequent screening results are analyzed using a UV-VIS spectrophotometer. The test is repeated three times.

#### Dissolution Test:

The dissolution test uses the paddle method with a USP type II dissolution apparatus. 50mg of CA, CA PM, and CA CC samples are dissolved in 900ml of phosphate buffer media (pH = 6.6) and stirred at 75 rpm at a temperature of 37±0.2°C. A total of 5 mL of dissolution media is collected at 5 minutes, 10 minutes, 15 minutes, 30 minutes, 45 minutes, and 60 minutes after the end of stirring and replaced with the same volume of fresh media. The subsequent screening results are analyzed using a UV-VIS spectrophotometer. The test is repeated three times.

#### Computation Investigation Using QTAIM of Bader:

Optimization of molecular geometry for active pharmaceutical ingredients (APIs), cofomers, and cocrystals is computed using Density Functional Theory (DFT) method with Gaussian16 program, employing Yang-Parr exchange correlation functional theory (B3LYP) and basis set 6-311++G(d,p)<sup>28</sup>. The results of this optimization are then used to determine topology and non-covalent interaction energies using Multiwfn 3.8, which are subsequently visualized using Visual Molecular Dynamics (VMD) 1.9.4.

## RESULT:

### Cocrystalline CA-NIC synthesis:

The slow solvent evaporation method has successfully synthesised cinnamic acid and nicotinamide cocrystals, as shown in Figure 2.

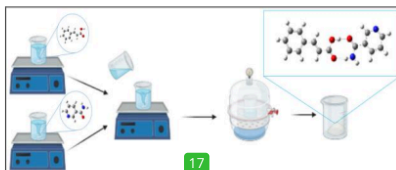


Figure 1. Synthesis pathway of co-crystals of cinnamic acid and nicotinamide using solvent evaporation method.

Figure 1 shows that the cocrystal synthesis process begins with dissolving cinnamic acid and nicotinamide in acetonitrile in a ratio of 1:1, respectively. Next, the two solutions were mixed with a stirring hot plate for 2 hours. The mixture was left in a desiccator for five days, and the solvent was slowly evaporated to reduce the concentration of the solution so that white crystals formed.

### Differential Scanning Calorimetry (DSC) Analysis:

DSC is used to identify properties of cocrystals where melting point changes indicate the formation of new phases or interactions between components of cocrystals. The results of the characterization of cinnamic acid and its cocrystals using DSC can be seen in Figure 2.

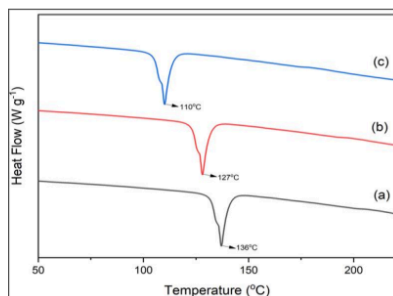


Figure 2. DSC curves for (a) Cinnamic acid, (b) Nicotinamide, and (c) Cocrystal of cinnamic acid

Figure 2 shows that cinnamic acid has endothermic peak was 136 °C, according to the research of Kopjar<sup>33</sup>, while nicotinamide conformer shows an endothermic peak was 127 °C, according to the research of Ding<sup>34</sup>. The cinnamic acid cocrystal showed the shift endothermic peak was 110°C.

6

**Powder X-ray Diffraction (PXRD) Analysis:**

Powder XRD is used to identify the phase of the cocrystal by detecting changes in the crystal lattice. Various cocrystals exhibit different characteristic peaks due to their unique crystal structures. The formation of cocrystals often leads to changes in the dimensions of the unit cell compared to the individual components. These changes are reflected in the PXRD pattern, which causes the appearance of new peaks or shifts in existing peaks.<sup>35</sup> PXRD results of cinnamic acid and its cocrystal can be seen in Figure 3.

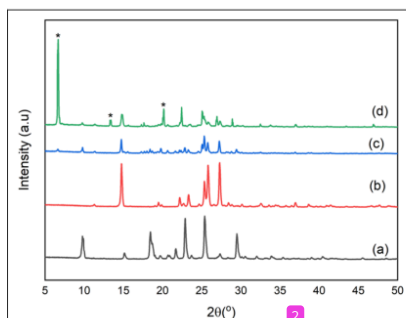


Figure 3. PXRD curve for (a) Cinnamic acid; (b) Nicotinamide; (c) Physical mixture and (d) Cocrystal of cinnamic acid

The results of XRD analysis in Figure 3 show that cinnamic acid has characteristic peaks at 9.8°, 14.8°, 18.5°, 22.9°, 25.4° and 29.5° as in the research of Trivedi<sup>36</sup>. Nicotinamide has characteristic peaks at 14.8°; 22.2°; 27.3°; 25.4°; 25.8°; and 27.3° as reported by Junior<sup>37</sup>. On the other hand, the physical mixture between cinnamic acid and nicotinamide showed peaks at 9.8°, 22.9° and 25.4° from the characteristic peak of cinnamic acid and 14.8°, 22.2°, 23.3°, 25.8° and 27.3° from nicotinamide. This shows that no new crystalline phase is formed in the physical mixture, and only a mixture of cinnamic acid and nicotinamide is formed individually. The cocrystal shows a new crystalline phase formation indicated by characteristic peaks at 6.7°, 13.4° and 20.2°. In comparison, there are peaks of individual cinnamic acid that are lost at 9.8° and 18.5°, and the peaks of the missing individual nicotinamide are 22.2° and 23.3°.

**Attenuated Total Reflectance-Fourier Transform Infrared (ATR-FTIR) Analysis:**

The cocrystallization was characterized using ATR-FTIR due to its ability to provide detailed information about the molecular structure and intermolecular interactions within the cocrystal lattice. The results of ATR-FTIR characterization of cinnamic acid and its cocrystals can be seen in Figure 4.

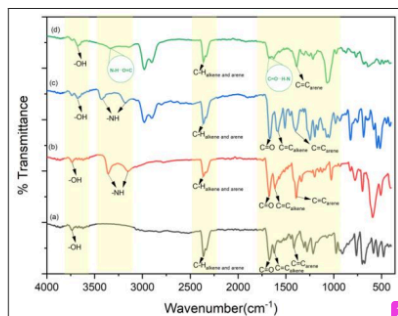


Figure 4. Infrared Spectra for (a) Cinnamic acid; (b) Nicotinamide; (c) Physical mixture and (d) Cocrystal of cinnamic acid

The FTIR characteristic results of cinnamic acid showed the stretching vibrations of -OH, -CH, -C=O, C=C<sub>alkene</sub> and C=C<sub>arene</sub> at 3739 cm<sup>-1</sup>, 2361 cm<sup>-1</sup>, 1669 cm<sup>-1</sup>, 1620 cm<sup>-1</sup> and 1414 cm<sup>-1</sup>, respectively, as in previous studies<sup>8,36,38</sup>. On the other hand, nicotinamide showed stretching vibration of -OH, -NH, -C=O, C=C<sub>alkene</sub> and C=C<sub>arene</sub> at wavelengths of 3736 cm<sup>-1</sup>; 3426 cm<sup>-1</sup> and 3182 cm<sup>-1</sup>, 2361 cm<sup>-1</sup>; 1674 cm<sup>-1</sup>; 1614 cm<sup>-1</sup> and 1391 cm<sup>-1</sup>, respectively, as in previous studies<sup>37</sup>. In addition, the physical mixture between cinnamic acid and nicotinamide shows absorption peaks which are a combination of individuals, stretching vibration of -OH, -NH, -C=O, C=C<sub>alkene</sub> and C=C<sub>arene</sub> at wavelengths of 3677 cm<sup>-1</sup>, 3426 cm<sup>-1</sup> and 3182 cm<sup>-1</sup>, 2361 cm<sup>-1</sup>, 1668 cm<sup>-1</sup>, 1585 cm<sup>-1</sup>, and 1398 cm<sup>-1</sup>. The cocrystal shows the same peaks as API and coformers, stretching vibration of -OH, -CH, and C=C<sub>arene</sub> at wavelengths of 3674 cm<sup>-1</sup>; 2361 cm<sup>-1</sup>; and 1389 cm<sup>-1</sup> but there is a missing stretching vibration of -NH and fusion-like absorption peaks of -C=O and -C=C alkene.

**Scanning Electron Microscopy (SEM) Analysis:**

SEM characterized the cocrystals to understand their morphology, which is essential for assessing their physical and behavioural properties. The results of the characterization of cinnamic acid and its cocrystals by SEM can be seen in Figure 5. Figure 6 shows that SEM results indicate that cinnamic acid has an irregular plate-like shape, as in Batista<sup>39</sup> and Silva<sup>38</sup> studies. On the other hand, the cocrystals that are formed have a smooth surface morphology and regular block-like shape, which differs from the individual API. In addition, SEM results show a difference in crystal size; for cinnamic acid, the size is 44.93 μm and the cocrystal is 20.18 μm.

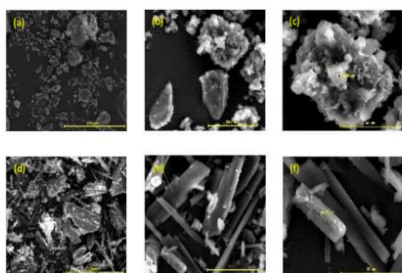


Figure 5. SEM morphology for cinnamic acid (above) observation with: (a) 500x (b) 2500x (c) 5000x and co-crystallization (below) observation with: (d) 500x (e) 2500x (f) 5000x

**Solubility Test:**

Solubility tests showed that the solvent-evaporated co-crystals had higher solubility values than cinnamic acid and the physical mixture, as shown in Figure 6.

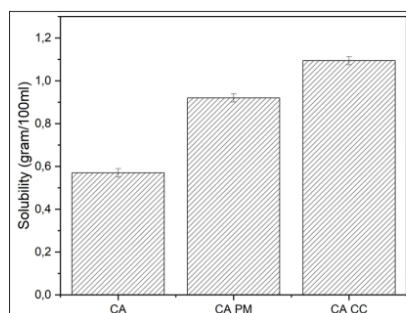


Figure 6. Solubility Test Profile: cinnamic acid (CA), physical mixture (CA PM), and co-crystal (CA CC)

Figure 6 shows that the highest solubility in order was found in co-crystals, physical mixture, and cinnamic acid. The solubility of cinnamic acid was 0.57 g/100 ml, the physical mixture was 0.92 g/100 ml, and the co-crystal was 1.09 g/100 ml.

**Dissolution Test:**

Dissolution tests showed that the co-crystals had a higher dissolution rate than cinnamic acid and the physical mixture, as shown in Figure 7. Figure 6 shows that the dissolution test results indicate that the co-crystal of cinnamic acid with nicotinamide by solvent evaporation has the highest rate compared to the physical mixture and individual cinnamic acid. Cinnamic acid showed a DE of 80.104%, while the physical mixture showed a slight increase with a DE of 87.284%. The co-crystal had the highest DE value of 96.021%.

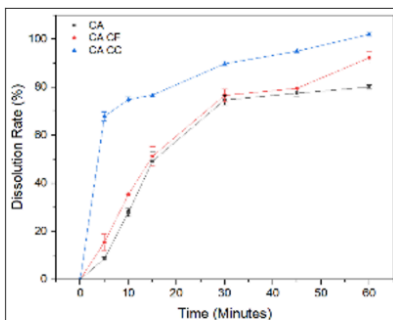


Figure 7. Dissolution rate profiles of cinnamic acid (CA), physical mixture (CA PM), and co-crystal (CA CC)

**Computation Investigation Using QTAIM of Bader:**

Topology and noncovalent interaction energy analysis tests of cinnamic acid and Nicotinamide co-crystals were performed using the Quantum Theory Atom In Molecules of Bader (QTAIM) method. The use of such QTAIM method to analyze the topology and energy of noncovalent interactions in co-crystals is driven by its ability to provide a detailed, quantitative, and comprehensive understanding of intermolecular interactions, which is important for fundamental research and practical applications in crystal engineering e.g. solubility properties<sup>32</sup>. The results of topological analysis of cinnamic acid and Nicotinamide co-crystals are shown in Figure 8.

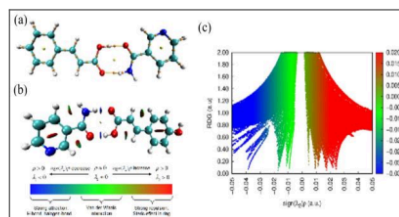


Figure 8. Topological analysis results of the co-crystal of cinnamic acid and Nicotinamide using the QTAIM method: (a) Molecular Geometry, (b) Isosurface Map, (c) Red Density Gradient (RDG) (blue = hydrogen bond; green = van der Waals bond; Red = Steric Effect)

Figure 8 (a) shows that the topological results of QTAIM analysis indicate that co-crystals of cinnamic acid and nicotinamide are formed with the presence of intermolecular bonds between the carboxylic group of cinnamic acid with the amide group of nicotinamide and between the hydroxide group of cinnamic acid with the carboxylic group of nicotinamide. On the other hand, the isosurface map in Figure 9 (b) shows that the bonds that

occur in the formation of cocrystals are hydrogen bonds indicated by blue chips. This result is also supported by Figure 9 (c), where there is a blue spike in  $\text{sign}(\lambda_2)\rho$  around -0.04 a.u., which indicates the presence of hydrogen bonds<sup>31</sup>. The topology results<sup>34</sup> are also supported by quantitative QTAIM analysis in Table 1.

Table 1 shows that the cocrystals of cinnamic acid and nicotinamide  $\nabla^2\rho(r)$  of 0.1195 a.u. and 0.1282 a.u.,  $H(r)$  of 0.0092 a.u. and 0.0201 a.u., and  $|V(r)|/G(r)$  of 0.0599 a.u. and 0.1004 a.u. which indicates the interactions that occur are intermolecular hydrogen bonds. The hydrogen bond has an interaction energy of -76.0833 kcal/mol and an intermolecular hydrogen bond energy of -63.525 kJ/mol and -95.025 kJ/mol.

## DISCUSSION:

In this study, cocrystallization has been carried out with the active ingredients ferulic acid and nicotinamide as cofomers through the methanol solvent evaporation method. As shown in Figure 1, the cocrystal synthesis process begins with dissolving cinnamic acid and nicotinamide in acetonitrile until a clear solution is formed. Next, the two solutions were mixed and stirred for 2 hours, forming a clear solution. The mixture was left in a desiccator for five days to form white crystals. The white crystals were formed because as the solvent evaporated, the supersaturated solution finally reached the point where the first nucleation was formed. The subsequent growth of these nuclei into larger crystals is driven by the continued evaporation of the solvent and the ongoing intermolecular interactions between the drug molecules and the cofomer<sup>40-42</sup>. On the other hand, at the supersaturated state, the API molecules and the cofomer interact through intermolecular forces such as hydrogen bonding, ionic interactions, or  $\pi$ - $\pi$  stacking. These interactions facilitate the formation of a stable cocrystal lattice structure, i.e., white crystals<sup>43-46</sup>. The crystals were further characterized for their thermal properties by DSC, crystal structure by PXRD, functional groups by FTIR and morphology by SEM.

The DSC results in Figure 3 show that the melting temperature of the formed cocrystals is lower than that of the API and individual conformers. This is due to

stronger intermolecular interactions and supramolecular heterosinones, and the increased thermodynamic stability of the cocrystals contributes to the formation of more stable cocrystals with lower melting points<sup>44,47</sup>. The lower melting point indicates that the cocrystal has a lower energy level than the individual components, which is due to stronger intermolecular interactions in the cocrystal lattice<sup>48-50</sup>. This is also supported by the difference in PXRD diffractogram patterns between cinnamic acid and its cocrystal, as shown in Figure 4. The characteristic diffractogram patterns observed in the XRD results of the samples at 6.7°, 13.4°, and 20.2° result from the unique crystal lattice structure and intermolecular interactions in the cocrystal. The formation of new peaks indicates a change in the dimensions of the unit cell and the appearance of new intermolecular interactions not seen in the individual components<sup>47,51-54</sup>.

The FTIR characterization also supports the PXRD and DSC results in Figure 5. The formation of cocrystals from FTIR results occurs due to the disappearance of twin peaks at wave numbers around 3400-3000  $\text{cm}^{-1}$  of the -NH group caused by strong hydrogen bonds between the amide group of nicotinamide and the carboxyl group of cinnamic acid while the appearance of fusion-like peaks at wavenumbers around 1600  $\text{cm}^{-1}$  and 1500  $\text{cm}^{-1}$  indicating of -C=O and -C=C<sub>alkene</sub> is caused by the formation of new bonds and changes in the bonding environment in the cocrystal lattice as the results of PXRD<sup>47,54-57</sup>. The results of these characterizations are also supported by SEM morphology and the size of solids that differ between cinnamic acid and cocrystals, as shown in Figure 6. SEM results show that cinnamic acid has an irregular plate-like shape, as in the studies of Batista<sup>39</sup> and Silva<sup>38</sup>, while the cocrystals formed have a smooth surface morphology and a regular block-like shape. On the other hand, the size of the cinnamic acid crystal is 44.93  $\mu\text{m}$ , and the cocrystal is 20.18  $\mu\text{m}$ . This is due to the new intermolecular interactions introduced by the cofomer, which result in changes in particle shape and size so that the morphology of the cocrystal is different from that of individual cinnamic acid<sup>24,58</sup>.

Table 1. The topological parameters obtained from the QTAIM analysis

Material	$E_{int}$ (Kcal/mol)	$\dagger$ BCP	$\rho$ (a.u.)	$\nabla^2\rho$ (a.u.)	G (a.u.)	H (a.u.)	V (a.u.)	$E_{H\cdots O}$ (kJ/mol)	$\epsilon$ (a.u.)
CA CC	-76.083	C=O <sub>CA</sub> ...N <sub>CC</sub> H-N	0.0383	0.1195	0.0391	0.0092	-0.0484	-63.525	0.0054
		O-H <sub>CA</sub> ...N <sub>CC</sub> O=C	0.0562	0.1282	0.0522	0.0201	-0.0724	-95.025	0.0021

$\dagger$ Bond Critical Point (BCP), energy interaction ( $E_{int}$ )/electron density ( $\rho$ ), Laplacian of electron density ( $\nabla^2\rho$ ), Lagrangian kinetic energy (G), Hamiltonian kinetic energy (H), Potential energy density (V), Hydrogen bond Energy (EH...O), and ellipticity of electron density

Previous research<sup>8,35,59,60</sup> showed that cocrystals can increase solubility and dissolution compared to API due to differences in structure and physicochemical properties between cocrystals and API. This is in line with this study in Figure 7, where the solubility of cinnamic acid is 0.57g/100 ml. After being synthesized into cocrystals, the solubility increases 1.91 times to 1.09g/100 ml due to strong intermolecular interactions and a denser and more ordered cocrystal lattice structure. These interactions increase solubility by improving the interaction with the solvent and reducing the energy required for dissolution<sup>8,45,61,62</sup>. This is by the parachute spring effect, whereby when a drug forms a cocrystal with a conformer, new intermolecular interactions are introduced that can loosen or alter the crystal lattice. These changes in intermolecular bonds increase the solubility of the drug by making it easier for the solvent to penetrate and dissolve it like a spring. The stability of the cocrystal will make the solubility stability sustainable, like a parachute, to increase the effectiveness of the drug in the body<sup>46,63</sup>. On the other hand, the dissolution rate of cocrystals, as shown in Figure 8, is higher when compared to individual cinnamic acid and its physical mixture, where cinnamic acid shows a Dissolution Efficiency (DE) of 80.104% after becoming a cocrystal, the DE value increases to 96.021%. This is because cocrystals are formed through intermolecular interactions that stabilize the cocrystal lattice and create a more regular structure. This increased orderliness increases the rate at which the cocrystal solubilizes by providing a more favourable environment for the solvent molecules to interact with the drug molecules. This result is also proven by the magnitude of the drug dissolution rate, which is directly proportional to the solubility of the drug<sup>60</sup>.

The intermolecular bonds of the cocrystals were predicted using the QTAIM method, as shown in Figure 9 and Table 1. The use of such a method is because it provides a detailed and quantitative analysis of the noncovalent interactions that stabilize these complexes and can gain a thorough understanding of the intermolecular interactions that stabilize the cocrystals, which is crucial for predicting their solubility, dissolution rate and overall stability<sup>28,31,64,65</sup>. Figure 9 shows that the cocrystals of cinnamic acid and nicotinamide are formed by the intermolecular bond between the carboxylic group of cinnamic acid with the amide group of nicotinamide on the  $C=O_{CA} \cdots N_{IC}H-N$  synthon<sup>69</sup> and between the hydroxide group of cinnamic acid with the carboxylic group of nicotinamide on the  $O_{H_{CA}} \cdots N_{IC}O=C$  synthon. On the other hand, based on the isosurface map shows that the bonds that occur in the cocrystal formation are hydrogen bonds indicated by blue colour chips supported by the RDG Scatter Plot where there is a blue spike at sign  $(\lambda_2)\rho$  around -0.04 a.u as research by Pujiono<sup>31</sup>.

The topological parameter results from QTAIM predict that intermolecular hydrogen bonds are formed if  $\nabla_2\rho(r) > 0$ ,  $H(r) > 0$ , and  $|V(r)|/G(r) < 1$  as reported by Hammami and Issaoui<sup>66</sup>. The report supports the results of this study, shown in Table 1, that the interactions that occur in cocrystal formation are intermolecular hydrogen bonds. In addition, these results are also supported by Espinosa's postulates<sup>65-68</sup> where if there is hydrogen bonding, the Laplacian value is 0.024-0.139 a.u while the results of this study are 0.1195 a.u and 0.1282 a.u Laplacian values. Hydrogen bonds between cocrystal molecules and solvents can increase solubility and dissolution because cocrystals containing hydrogen bond acceptors such as oxygen or nitrogen atoms can form hydrogen bonds with water molecules, making it easier for cocrystals to dissolve in water<sup>69-72</sup>.

#### CONCLUSION:

Cinnamic acid cocrystals have been synthesized with nicotinamide conformer by a solvent evaporation method. The synthesis results obtained white crystals, and characterization results show that the crystals are cinnamic acid-nicotinamide cocrystals. Characterization results with DSC show that cinnamic acid cocrystals have an endothermic peak (110°C) in contrast to cinnamic acid (136°C) and individual nicotinamide (127°C). These results are also supported by the results of PXRD, where cinnamic acid cocrystals have different diffractogram patterns with cinnamic acid and individual nicotinamide as well as with physical mixtures, the presence of diffractogram peaks at 6.7°, 13.4° and 20.2°. On the other hand, the results of FTIR characterization also show that cinnamic acid cocrystals have different FTIR spectra, the disappearance of twin peaks at wave numbers around 3400-3000  $cm^{-1}$  from the -NH group and absorption peaks that are fusion-like at wave numbers around 1600  $cm^{-1}$  and 1500  $cm^{-1}$ , indicating  $C=O$  and  $C=C_{alkene}$  and SEM results which show different SEM morphology and solid size between cinnamic acid and cocrystals. SEM results show that cinnamic acid has an irregular plate-like shape as the research, while the cocrystals formed have a smooth face morphology and an irregular block-like shape. On the other hand, the crystal size of cinnamic acid is 44.93mm, and the cocrystal is 20.18mm. The solubility test showed that the solubility of cinnamic acid was 0.57 g/100ml. After being synthesized into cocrystals, the solubility rose 1.91 times to 1.09g/100ml. The solubility test is directly proportional to the dissolution test; cinnamic acid shows a Dissolution Efficiency (DE) of 80.104% after becoming a cocrystal, and the DE value increases to 96.021%. QTAIM topology results, cinnamic acid and nicotinamide cocrystals are formed by the presence of intermolecular bonds between the carboxylic group of cinnamic acid with the amide group of nicotinamide on the  $C=O_{CA} \cdots N_{IC}H-N$  synthon and

28

between the hydroxide group of cinnamic acid with the carboxylic group of nicotinamide on the  $O-H_{CA} \cdots N_{NIC}O=C$  synthon. Based on the isosurface map, it shows that the bonds that occur in the cocrystal formation are hydrogen bonds indicated by blue colour chips supported by the RDG Scatter Plot where there is a blue spike at  $\text{sign}(\lambda_2)$  around  $-0.04$  a.u.

19

#### CONFLICT OF INTEREST:

The authors have no conflicts of interest regarding this investigation.

23

#### KNOWLEDGMENTS:

The authors would like to thank Institut Ilmu Kesehatan Bhakti Wiyata, Bhakti Wiyata Foundation and Airlangga University support during studies.

#### REFERENCES:

- Harahap FS, Marpaung H. Perbandingan Kandungan Asam Sinamat Dan Asam Benzoat Dalam Kemeyan (Styrax Benzoin) Kualitas I, Iii Dan V Yang Diperoleh Dari Daerah Tapanuli Utara Dengan Metode Kromatografi Gas. 2018; 3: 42-7. <https://doi.org/https://doi.org/10.24114/ijest.v7i1.56438>
- Riyanto A, Yunilawati R, Nuraeni C. Isolasi Metil Sinamat dari Minyak Atsiri Laja Gowah (Alpinia malaccensis (Burm. f.)). *Jurnal Kimia dan Kemasan*. 2012; 34: 237-42. <https://doi.org/https://doi.org/10.24817/jkk.v34i2.1859>
- Youn I, Han AR, Piao D, Lee H, Kwak H, Lee Y, et al. Phytochemical and pharmacological properties of the genus *Alpinia* from 2016 to 2023. *Nat Prod Rep*. 2024; <https://doi.org/https://doi.org/10.1039/d4np00004h>
- Zeng L, Wang X, Tan H, Liao Y, Xu P, Kang M, et al. Alternative pathway to the formation of trans-cinnamic acid derived from L-phenylalanine in tea (*Camellia sinensis*) plants and other plants. *J Agric Food Chem*. 2020; 68: 3415-24. <https://doi.org/https://doi.org/10.1021/acs.jafc.9b07467>
- Manogaran Y, Jagadeesan D, Namin K, Kuman U, Anand P, Shanmugavelu S. Antibacterial Response of Cinnamomum iners Leaves Extract and Cinnamic Acid Derivative against Pathogens that Triggers Periapicalitis. *Res J Pharm Technol*. 2023; 1471-80. <https://doi.org/10.52711/0974-360X.2023.00242>
- Wang Y, Sun Y, Wang J, Zhou M, Wang M, Feng J. Antifungal activity and action mechanism of the natural product cinnamic acid against *Sclerotinia sclerotiorum*. *Plant Dis*. 2019; 103: 944-50. <https://doi.org/https://doi.org/10.1094/PDIS-08-18-1355-RE>
- Li H, Ma Y, Gao X, Chen G, Wang Z. Probing the structure-antioxidant activity relationships of four cinnamic acids porous starch esters. *Carbohydr Polym*. 2021; 256: 117428.
- dos Santos JAB, Chaves Júnior JV, de Araújo Batista RS, de Sousa DP, Ferreira GLR, de Lima Neto SA, et al. Preparation, physicochemical characterization and solubility evaluation of pharmaceutical cocrystals of cinnamic acid. *J Therm Anal Calorim*. 2021; 145: 379-90.
- Feng L, Cheng J, Su W, Li H, Xiao T, Chen D, et al. Cinnamic acid hybrids as anticancer agents: A mini-review. *Arch Pharm (Weinheim)*. 2022; 355: 2200052. <https://doi.org/https://doi.org/10.1002/ardp.202200052>
- Das B, Baidya ATK, Mathew AT, Yadav AK, Kumar R. Structural modification aimed for improving solubility of lead compounds in early phase drug discovery. *Bioorg Med Chem*. 2022; 116614. <https://doi.org/https://doi.org/10.1002/ardp.202200052>
- Sopyan I, Gozali D, Megantara S, Wahyuningrum R, KS IS. AN Efforts To Increase The Solubility and Dissolution of Active Pharmaceutical Ingredients. *Int J App Pharm*. 2022; 14: 22-7. <https://doi.org/https://doi.org/10.22159/ijap.2022v14i1.43431>
- Jit T, Shil D, Kuman Dasgupta R, Mallick S, Mukherjee S. Cocrystal: A Review on the Design and Preparation of Pharmaceutical Cocrystals. *Asian Journal of Research in Pharmaceutical Sciences*. 2023; 296-302. <https://doi.org/10.52711/2231-5659.2023.00050>
- Vyas G, Jigar S, Jacob S. Enhancement of Physicochemical and Pharmacokinetic Characteristics of Ranolazine drug substance using Cocrystallization Technique. *Res J Pharm Technol*. 2024; 59-66. <https://doi.org/10.52711/0974-360X.2024.00010>
- Dutt B, Choudhary M, Budhwar V. Enhancement of Stability profile of Aspirin through Cocrystallization Technique. *Res J Pharm Technol*. 2022; 768-72. <https://doi.org/10.52711/0974-360X.2022.00128>
- Budiman A, Megantara S, Saraswati P. Synthesize Glibenclamide-Ascorbic Acid Cocrystal Using Solvent Evaporation Method to Increase Solubility and Dissolution Rate of Glibenclamide. *Res J Pharm Technol*. 2019; 12: 5805. <https://doi.org/10.5958/0974-360X.2019.01005.9>
- Wisudyaningih B, Sallama S, Siswandono S, Setyawan D. The Effect of pH and Cocrystal Quercetin-Isonicotinamide on Quercetin Solubility and its Thermodynamic. *Res J Pharm Technol*. 2021; 4657-61. <https://doi.org/10.52711/0974-360X.2021.00809>
- J T, NN S, Raheem T A, SKK S, G T. Modafinil Cocrystals for Altered Physicochemical Properties. *Res J Pharm Technol*. 2021; 4891-6. <https://doi.org/10.52711/0974-360X.2021.00850>
- Fael H, Barbas R, Prohens R, Ráfols C, Fuguet E. Synthesis and characterization of a new norfloxacin/resorcinol cocrystal with enhanced solubility and dissolution profile. *Pharmaceutics*. 2021; 14: 49. <https://doi.org/https://doi.org/10.3390/pharmaceutics14010049>
- Duan C, Liu W, Tao Y, Liang F, Chen Y, Xiao X, et al. Two novel paltociclib-resorcinol and paltociclib-orscinol cocrystals with enhanced solubility and dissolution rate. *Pharmaceutics*. 2021; 14: 23. <https://doi.org/https://doi.org/10.3390/pharmaceutics14010023>
- Sabouri S, Shayanfar A. Effects of Surfactant and Polymer on Thermodynamic Solubility and Solution Stability of Carbamazepine-Cinnamic Acid Cocrystal. *Pharm Chem J*. 2022; 56: 913-7. <https://doi.org/https://doi.org/10.1007/s11094-022-02726-8>
- Hiendrawan S, Veriansyah B, Tjandrawinata R. Solid-state properties and solubility studies of novel pharmaceutical cocrystal of itraconazole. *International Journal of Applied Pharmaceutics*. 2018; 10: 97-104. <https://doi.org/https://doi.org/10.22159/IJAP.2018V10I5.26663>
- Pawar RR, Nahire SB. Investigation, correlation and DFT study for solubility of malonic acid in water + methanol and water + ethanol binary solvents at T = 293.15 to 313.15 K. *Res J Pharm Technol*. 2021; 14: 1226-32. <https://doi.org/10.5958/0974-360X.2021.00218.3>
- Ghamamy S, Qaitmas NA, Lashgari A. Structural Properties, Natural Bond Orbital, Theory Functional Calculations (DFT), and Energies for the Two New Halo Organic Compounds. *Asian Journal of Research in Chemistry*. 2015; 8: 60. <https://doi.org/10.5958/0974-4150.2015.00013.9>
- Ali A, Kuznetsov A, Ibrahim M, Abbas A, Akram N, Maqbool T. Chemistry and modern techniques of characterization of Cocrystals. In: *Drug Formulation Design*. IntechOpen; 2022. <https://doi.org/https://doi.org/10.5772/intechopen.108694>
- Majumdar D, Philip JE, Tüzün B, Frontera A, Gomila RM, Roy S, et al. Unravelling the synthetic mimic, spectroscopic insights, and supramolecular crystal engineering of an innovative heteronuclear Pb (II)-salen cocrystal: an integrated DFT, QTAIM/NCI Plot, NLO, molecular docking/PLIP, and antibacterial appraisal. *J Inorg Organomet Polym Mater*. 2022; 32: 4320-39. <https://doi.org/https://doi.org/10.1007/s10904-022-02448-0>
- Dey P, Islam S, Das P, Seth SK. Structural and computational insights into two trimethylenedipyridine co-crystals: Inputs from

- X-ray diffraction, Hirshfeld surface, PIXEL, QTAIM and NCI plots. *J Mol Struct.* 2024; 1296: 136820. <https://doi.org/https://doi.org/10.1016/j.molstruc.2023.136820>
27. Pokharia S. An Atoms-in-molecules (AIM) interpretation of organotin-peptide system: I. Di-*n*-butyltin(IV) derivative of glycyltryptophane. *Asian Journal of Research in Chemistry.* 2017; 10: 115. <https://doi.org/10.5958/0974-4150.2017.00017.7>
  28. Huang S, Cheemarla VKR, Tiana D, Lawrence SE. Experimental and theoretical investigation of hydrogen-bonding interactions in cocrystals of sulfaguanidine. *Cryst Growth Des.* 2023; 23: 2306–20. <https://doi.org/https://doi.org/10.1021/acs.cgd.2c01337>
  29. Muthusamy AR, Singh A, Sundaram MSS, Wagh Y, Jegorov A, Jain AK. In-silico aided screening and characterization results in stability enhanced novel roxadustat co-crystal. *J Pharm Sci.* 2024; 113: 1190–201. <https://doi.org/https://doi.org/10.1016/j.xphs.2023.10.024>
  30. Yadav B, Balasubramanian S, Chavan RB, Thipparaboina R, Naidu VGM, Shastri NR. Hepatoprotective cocrystals and salts of riluzole: prediction, synthesis, solid state characterization, and evaluation. *Cryst Growth Des.* 2018; 18: 1047–61. <https://doi.org/https://doi.org/10.1021/ACS.CGD.7B01514>
  31. Pujiono FE, Setyawan D, Ekowati J. Hydrogen bond analysis of the p-coumaric acid-nicotinamide cocrystal using the DFT and AIM method. *Pharmacy Education.* 2024; 24: 57–62. <https://doi.org/https://doi.org/10.46542/pe.2024.243.5762>
  32. Yadav A, Chaudhary R, Bahota AS, Prajapati P, Pandey J, Narayan A, et al. Combined spectroscopic and quantum chemical study to explore the effect of hydrogen bonding in hydrochlorothiazide-nicotinamide cocrystal. *J Mol Struct.* 2024; 1300: 137208. <https://doi.org/https://doi.org/10.2139/ssrn.4387023>
  33. Kojar M, Buljeta I, Jelić I, Kelemen V, Šimunović J, Pichler A. Encapsulation of cinnamic acid on plant-based proteins: Evaluation by HPLC, DSC and FTIR-ATR. *Plants.* 2021; 10: 2158. <https://doi.org/https://doi.org/10.3390/plants10102158>
  34. Ding Y, Zhao T, Fang J, Song J, Dong H, Liu J, et al. Recent developments in the use of nanocrystals to improve bioavailability of APIs. *Wiley Interdiscip Rev Nanomed Nanobiotechnol.* 2024; 16: e1958. <https://doi.org/https://doi.org/10.1002/wnan.1958>
  35. Setyawan D, Sulistyowaty MI, Sari IP, Yusuf H, Zaini E. The formation of p-Methoxycinnamic acid-caffeine co-crystal by the solution evaporation method and its physicochemical characterization. In: *AIP Conference Proceedings.* AIP Publishing; 2023. <https://doi.org/https://doi.org/10.1063/5.0119975>
  36. Trivedi HR, Borkar DS, Puranik PK. Experimental design approach for development of cocrystals and immediate release cocrystal tablet of atorvastatin calcium for enhancement of solubility and dissolution. *Journal of Research in Pharmacy.* 2020; 24: 720–37. <https://doi.org/https://doi.org/10.35333/jrp.2020.226>
  37. Júnior JVC, Dos Santos JAB, Lins TB, de Araújo Batista RS, de Lima Neto SA, de Santana Oliveira A, et al. A new ferulic acid-nicotinamide cocrystal with improved solubility and dissolution performance. *J Pharm Sci.* 2020; 109: 1330–7.
  38. Silva JRA, da Cunha Holanda BB, e Silva GT de S, Moraes CRP, Barbosa TWL, dos Santos EM, et al. Gemfibrozil-trans-cinnamic acid co-crystal: Synthesis, characterization, in vitro solubility and cell viability studies. *J Appl Pharm Sci.* 2023; 13: 18–26. <https://doi.org/https://doi.org/10.7324/japs.2023.93828>
  39. Batista RS de A, Melo TBL, dos Santos JAB, de Andrade FHD, Macedo RO, de Souza FS. Evaluation of crystallization technique relating to the physicochemical properties of cinnamic acid. *J Therm Anal Calorim.* 2019; 138: 3727–35. <https://doi.org/https://doi.org/10.1007/s10973-019-08455-7>
  40. Bolla G, Sarma B, Nangia AK. Crystal engineering and pharmaceutical crystallization. In: *Hot topics in crystal engineering.* Elsevier; 2021. p. 157–229. <https://doi.org/https://doi.org/10.1016/B978-0-12-818192-8.00004-4>
  41. Sultan M, Wu J, Haq IU, Imran M, Yang L, Wu J, et al. Recent progress on synthesis, characterization, and performance of energetic cocrystals: A review. *Molecules.* 2022; 27: 4775. <https://doi.org/https://doi.org/10.3390/molecules27154775>
  42. Sarangi S, Remya PN, Damodharan N. Advances in solvent based cocrystallization: Bridging the gap between theory and practice. *J Drug Deliv Sci Technol.* 2024; 105619. <https://doi.org/https://doi.org/10.1016/j.jddst.2024.105619>
  43. Karimi-Jafari M, Padrela L, Walker GM, Croker DM. Creating cocrystals: A review of pharmaceutical cocrystal preparation routes and applications. *Cryst Growth Des.* 2018; 18: 6370–87. <https://doi.org/https://doi.org/10.1021/acs.cgd.8b00933>
  44. Thayyil AR, Juturu T, Nayak S, Kamath S. Pharmaceutical cocrystallization: Regulatory aspects, design, characterization, and applications. *Adv Pharm Bull.* 2020; 10: 203. <https://doi.org/https://doi.org/10.34172/apb.2020.024>
  45. Bolla G, Sarma B, Nangia AK. Crystal engineering of pharmaceutical cocrystals in the discovery and development of improved drugs. *Chem Rev.* 2022; 122: 11514–603. <https://doi.org/https://doi.org/10.1016/B978-0-12-818192-8.00004-4>
  46. Wong SN, Fu M, Li S, Kwok WTC, Chow S, Low KH, et al. Discovery of new cocrystals beyond serendipity: lessons learned from successes and failures. *CrystEngComm.* 2024; <https://doi.org/https://doi.org/10.1039/D4CE00021H>
  47. Sakhiya DC, Borkhataria CH. A review on advancement of cocrystallization approach and a brief on screening, formulation and characterization of the same. *Heliyon.* 2024; <https://doi.org/https://doi.org/10.1016/j.heliyon.2024.e29057>
  48. Kilinkissa OEY, Govender KK, Bāthori NB. Melting point–solubility–structure correlations in chiral and racemic model cocrystals. *Cryst Eng Comm.* 2020; 22: 2766–71. <https://doi.org/https://doi.org/10.1039/D0CE00014K>
  49. Liu L, Wang JR, Mei X. Enhancing the stability of active pharmaceutical ingredients by the cocrystal strategy. *Cryst Eng Comm.* 2022; 24: 2002–22. <https://doi.org/https://doi.org/10.1039/D1CE01327K>
  50. Ouyang J, Xing X, Yang B, Li Y, Xu L, Zhou L, et al. Terahertz spectroscopic characterization and DFT calculations of vanillin cocrystals with nicotinamide and isonicotinamide. *Cryst Eng Comm.* 2023; 25: 2038–51. <https://doi.org/https://doi.org/10.1039/D2CE01642G>
  51. Thayyil AR, Juturu T, Nayak S, Kamath S. Pharmaceutical cocrystallization: Regulatory aspects, design, characterization, and applications. *Adv Pharm Bull.* 2020; 10: 203. <https://doi.org/https://doi.org/10.34172/apb.2020.024>
  52. Voguri RS, Ranga S, Dey A, Ghosal S. Solid-State Phase Transition of Agomelatine-Phosphoric Acid Molecular Complexes along the Salt-Cocrystal Continuum: Ab Initio Powder X-Ray Diffraction Structure Determination and DFT-D2 Analysis. *Cryst Growth Des.* 2020; 20: 7647–57. <https://doi.org/https://doi.org/10.1021/acs.cgd.0c00752>
  53. Sopyan I, Alvin B, Insan Sunan KS, Megantara SA. Systematic review: co-crystal as efforts to improve physicochemical and bioavailability properties of oral solid dosage form. *Int J Appl Pharm.* 2021; 13: 43–52. <https://doi.org/10.22159/IJAP.2021V13I1.39594>
  54. Harichandana T, Reddy S, RAO A. Exploring cocrystals and polymorphism in pharmaceutical science: A comprehensive review. *International Journal of Science and Research Archive.* 2024; 12: 198–205. <https://doi.org/https://doi.org/10.30574/ijrsa.2024.12.1.0701>
  55. Garbacz P, Wesolowski M. Benzodiazepines co-crystals screening using FTIR and Raman spectroscopy supported by differential scanning calorimetry. *Spectrochim Acta A Mol Biomol Spectrosc.* 2020; 234: 118242. <https://doi.org/https://doi.org/10.1016/j.saa.2020.118242>
  56. Kamis MNA, Zaki HM, Anuar N, Jalil MN. Synthesis, characterization and morphological study of nicotinamide and p-coumaric acid cocrystal. *Indonesian Journal of Chemistry.* 2020; 20: 661–79. <https://doi.org/https://doi.org/10.22146/ijc.45530>

57. Xie Y, Zhou J, Zhang B, Zhang L, Yang D, Yang S, et al. Quality control of naringenin-carbamazepine drug-drug cocrystal: Quantitative analytical method construction of ATR-FTIR and Raman combined with chemometrics. *Microchemical Journal*. 2024; 202: 110774. <https://doi.org/https://doi.org/10.1016/j.microc.2024.110774>
58. Li Y, Zhang Y, Xu H, Li M, Li Z, Song Z, et al. Synthesis and characterization of supramolecular assembly probenecid cocrystal. *J Mol Struct*. 2024; 1298: 136786. <https://doi.org/https://doi.org/10.1016/j.molstruc.2023.136786>
59. Abdullah A, Mutmainnah M, Wikantyasning ER. Cocrystals of cefixime with nicotinamide: improved solubility, dissolution, and permeability. *Indonesian Journal of Pharmacy*. 2022; 394–400. <https://doi.org/https://doi.org/10.22146/ijp.2530>
60. Sulistyowaty MI, Setyawan D, Sari R, Paramanandana A, Maharani NA, Simorangkir TP. Preparation and Physicochemical Characterizations of p-Methoxycinnamic acid-Succinic Acid Cocrystal by Solvent Evaporation Technique. *Open Access Maced J Med Sci*. 2022; 10: 1444–9. <https://doi.org/https://doi.org/10.3889/oamjms.2022.10193>
61. Rathi N, Paradkar A, Gaikar VG. Polymorphs of curcumin and its cocrystals with cinnamic acid. *J Pharm Sci*. 2019; 108: 2505–16. <https://doi.org/https://doi.org/10.1016/j.xphs.2019.03.014>
62. Karagianni A, Malamatar M, Kachrimanis K. Pharmaceutical cocrystals: New solid phase modification approaches for the formulation of APIs. *Pharmaceutics*. 2018; 10: 18. <https://doi.org/https://doi.org/10.3390/pharmaceutics10010018>
63. Bavishi DD, Borkhataria CH. Spring and parachute: How cocrystals enhance solubility. *Progress in Crystal Growth and Characterization of Materials*. 2016; 62: 1–8. <https://doi.org/https://doi.org/10.1016/j.pcrysgrow.2016.07.001>
64. Martínez LM, Cruz-Angeles J, Vázquez-Dávila M, Martínez E, Cabada P, Navarrete-Bernal C, et al. Mechanical Activation by Ball Milling as a Strategy to Prepare Highly Soluble Pharmaceutical Formulations in the Form of Co-Amorphous, Co-Crystals, or Polymorphs. *Pharmaceutics*. 2022; 14: 2003. <https://doi.org/https://doi.org/10.3390/pharmaceutics14102003>
65. Carpio-Martínez P, Barquera-Lozada JE, Pendás AM, Cortés-Guzmán F. Laplacian of the Hamiltonian Kinetic Energy Density as an Indicator of Binding and Weak Interactions. *ChemPhysChem*. 2020; 21: 194–203. <https://doi.org/https://doi.org/10.1002/cpbc.201900769>
66. Hammami F, Issaoui N. A DFT study of the hydrogen bonded structures of pyruvic acid–water complexes. *Front Phys*. 2022; 10: 901736. <https://doi.org/https://doi.org/10.3389/fphy.2022.901736>
67. Espinosa E, Lecomte C, Molins E. Experimental electron density overlapping in hydrogen bonds: topology vs. energetics. *Chem Phys Lett*. 1999; 300: 745–8. [https://doi.org/https://doi.org/10.1016/S0009-2614\(98\)01399-2](https://doi.org/https://doi.org/10.1016/S0009-2614(98)01399-2)
68. Pendás AM, Francisco E, Suarez D, Costales A, Diaz N, Munárriz J, et al. Atoms in molecules in real space: a fertile field for chemical bonding. *Physical Chemistry Chemical Physics*. 2023; 25: 10231–62. <https://doi.org/https://doi.org/10.1039/d2cp05540f>
69. Xue N, He B, Jia Y, Yang C, Wang J, Li M. The mechanism of binding with the  $\alpha$ -glucosidase in vitro and the evaluation on hypoglycemic effect in vivo: Cocrystals involving synergism of gallic acid and conformer. *European Journal of Pharmaceutics and Biopharmaceutics*. 2020; 156: 64–74. <https://doi.org/https://doi.org/10.1016/j.ejpb.2020.08.024>
70. Guo M, Sun X, Chen J, Cai T. Pharmaceutical cocrystals: A review of preparations, physicochemical properties and applications. *Acta Pharm Sin B*. 2021; 11: 2537–64. <https://doi.org/10.1016/j.apsb.2021.03.030>
71. Guan D, Xuan B, Wang C, Long R, Jiang Y, Mao L, et al. Improving the physicochemical and biopharmaceutical properties of active pharmaceutical ingredients derived from traditional Chinese medicine through cocrystal engineering. *Pharmaceutics*. 2021; 13: 2160.
72. Bhatia M, Devi S. Co-crystallization: a green approach for the solubility enhancement of poorly soluble drugs. *Cryst Eng Comm*. 2024; 26: 293–311. <https://doi.org/https://doi.org/10.1039/d3ce01047c>

# Synthesis, Characterization and Dissolution Performance of Cocrystal of Cinnamic Acid with Nicotinamide: Experimental and Computation Investigation

## ORIGINALITY REPORT

15%

SIMILARITY INDEX

11%

INTERNET SOURCES

12%

PUBLICATIONS

%

STUDENT PAPERS

## PRIMARY SOURCES

1

[www.mdpi.com](http://www.mdpi.com)

Internet Source

2%

2

[journals.innovareacademics.in](http://journals.innovareacademics.in)

Internet Source

1%

3

[patentimages.storage.googleapis.com](http://patentimages.storage.googleapis.com)

Internet Source

1%

4

[www.researchsquare.com](http://www.researchsquare.com)

Internet Source

1%

5

Tobias N. Wassermann, Oleg V. Boyarkin, Béla Paizs, Thomas R. Rizzo. "Conformation-Specific Spectroscopy of Peptide Fragment Ions in a Low-Temperature Ion Trap", Journal of The American Society for Mass Spectrometry, 2012

Publication

1%

6

[link.springer.com](http://link.springer.com)

Internet Source

1%

7

Haoran Mei, Na Wang, Di Wu, Qi Rong, Xue Bai, Xin Huang, Lina Zhou, Ting Wang, Hongxun Hao. "Novel Pharmaceutical Cocrystals of Tegafur: Synthesis, Performance, and Theoretical Studies", Pharmaceutical Research, 2024

Publication

1%

8

[research.brighton.ac.uk](http://research.brighton.ac.uk)

Internet Source

<1%

9 Bouchra Chaib, Fayrouz Djellouli, Emine Berrin Poyraz. "A combined experimental and computational study of metronidazole and P-hydroxybenzoic acid cocrystal: QTAIM hydrogen-bond analysis, polymorphism screening and molecular docking", Pure and Applied Chemistry, 2026  
Publication

---

10 Meet Chhatbar, Chetan Borkhataria, Om Patel, Komal Raichura, Trupesh Pethani, Ghanshyam Parmar, Dhaval Mori, Ravi Manek. "Enhancing the Solubility and Bioavailability of Itraconazole through Pharmaceutical Cocrystallization: A Promising Strategy for Drug Formulation", Journal of Pharmaceutical Sciences, 2025  
Publication

---

11 s3-eu-west-1.amazonaws.com  
Internet Source

---

12 Cynthia A. Challener. "Chiral Drugs", Routledge, 2017  
Publication

---

13 Harita Desai, Nayan Gulhane, Gaurav Bhawe, Bandoo Chatale, Pranav Shah, Yahya I. Asiri, Mohd. Zaheen Hassan, Md. Faiyazuddin. "Mesalamine and Ascorbic Acid Drug-Drug Cocrystal-Loaded Suppositories: A Coadministrative Approach for Localized Treatment of Ulcerative Colitis", Journal of Pharmaceutical Innovation, 2025  
Publication

---

14 journal.umg.ac.id  
Internet Source

---

15 innovareacademics.in  
Internet Source

---

16	0-www-mdpi-com.brum.beds.ac.uk Internet Source	<1 %
17	Geetha Bolla, Bipul Sarma, Ashwini K. Nangia. "Crystal Engineering of Pharmaceutical Cocrystals in the Discovery and Development of Improved Drugs", Chemical Reviews, 2022 Publication	<1 %
18	journal.walisongo.ac.id Internet Source	<1 %
19	sciencescholar.us Internet Source	<1 %
20	www.codot.gov Internet Source	<1 %
21	Scott L. Childs, G. Patrick Stahly, Aeri Park. "The Salt-Cocrystal Continuum: The Influence of Crystal Structure on Ionization State", Molecular Pharmaceutics, 2007 Publication	<1 %
22	docslib.org Internet Source	<1 %
23	publichealthinafrica.org Internet Source	<1 %
24	www2.mdpi.com Internet Source	<1 %
25	Abdul Raheem Thayyil, Thimmasetty Juturu, Shashank Nayak, Shwetha Kamath. "Pharmaceutical Co-Crystallization: Regulatory Aspects, Design, Characterization, and Applications", Advanced Pharmaceutical Bulletin, 2020 Publication	<1 %
26	Kunal Chadha, Maninder Karan, Yashika Bhalla, Renu Chadha, Sadhika Khullar, Sanjay Mandal, Karan Vasisht. "Cocrystals of	<1 %

Hesperetin: Structural, Pharmacokinetic, and Pharmacodynamic Evaluation", Crystal Growth & Design, 2017

Publication

27

pspa.ff.unair.ac.id

Internet Source

<1 %

28

"Deep Eutectic Solvents", Springer Science and Business Media LLC, 2026

Publication

<1 %

29

Adam J. Smith, Padmini Kavuru, Lukasz Wojtas, Michael J. Zaworotko, R. Douglas Shytle. "Cocrystals of Quercetin with Improved Solubility and Oral Bioavailability", Molecular Pharmaceutics, 2011

Publication

<1 %

30

Suryanarayana Allu, Abhijit Garai, Vladimir V. Chernyshev, Ashwini K. Nangia. "Synthesis of Ternary Cocrystals, Salts, and Hydrates of Acefylline with Enhanced Dissolution and High Permeability", Crystal Growth & Design, 2022

Publication

<1 %

31

V.N. Vijayakumar, Sujay Chakravarty, S. Sundaram, T. Chitravel, V. Balasubramanian, R. Sukanya, A. Tharani. "HYDROGEN BOND THERMOTROPIC FERROELECTRIC LIQUID CRYSTAL OF DL-TARTARIC ACID AND 4-HEPTYLOXYBENZOIC ACID (1:1): EXPERIMENTAL AND DENSITY FUNCTIONAL THEORY (DFT) APPROACH", Journal of Molecular Structure, 2024

Publication

<1 %

32

Zimeng Wang, Hongzhou Shang, Linghuan Gao, Ning Qiao. "Research Progress of Plant Active Ingredients in Pharmaceutical Cocrystal", Current Drug Delivery, 2023

<1 %

---

33 ebin.pub <1 %  
Internet Source

---

34 perpustakaan.poltekkes-malang.ac.id <1 %  
Internet Source

---

35 pmc.ncbi.nlm.nih.gov <1 %  
Internet Source

---

36 pureadmin.qub.ac.uk <1 %  
Internet Source

---

37 Iman I. Soliman, Soha M. Kandil, Ebtsam M. Abdou. " Gabapentin-saccharin co-crystals with enhanced physicochemical properties and absorption formulated as oro-dispersible tablets ", Pharmaceutical Development and Technology, 2019 <1 %  
Publication

---

38 Lanting Zeng, Haibo Tan, Yinyin Liao, Guotai Jian, Ming Kang, Fang Dong, Naoharu Watanabe, Ziyin Yang. " Increasing Temperature Changes Flux into Multiple Biosynthetic Pathways for 2-Phenylethanol in Model Systems of Tea ( ) and Other Plants ", Journal of Agricultural and Food Chemistry, 2019 <1 %  
Publication

---

39 Mohamad Nor Amirul Azhar Kamis, Hamizah Mohd Zaki, Nornizar Anuar, Mohammad Noor Jalil Noor Jalil. "Preliminary assessment on cocrystals of nicotinamide:cinnamic acid and nicotinamide:p-coumaric acid at different solvents and ratio", Science Letters, 2021 <1 %  
Publication

---

40 Nao Ikeda, Yutaka Inoue, Yuka Ogata, Isamu Murata, Xuan Meiyang, Jun Takayama, Takeshi Sakamoto, Mari Okazaki, Ikuo Kanamoto. <1 %

"Improvement of the Solubility and Evaluation of the Physical Properties of an Inclusion Complex Formed by a New Ferulic Acid Derivative and  $\gamma$ -Cyclodextrin", ACS Omega, 2020

Publication

---

41 Noopur Rathi, Anant Paradkar, Vilas G. Gaikar. "Polymorphs of Curcumin and Its Cocrystals With Cinnamic Acid", Journal of Pharmaceutical Sciences, 2019 <1 %

Publication

---

42 Smita Suryawanshi, Parth Shaligram, Rajesh G. Gonnade, Sharvil Patil. "Novel Cocrystal of Quercetagenin: In vitro and in vivo Insights into Biopharmaceutical Performance", Pharmaceutical Research, 2026 <1 %

Publication

---

43 Structure and Bonding, 2012. <1 %

Publication

---

44 ecommons.cornell.edu <1 %

Internet Source

---

45 mdpi-res.com <1 %

Internet Source

---

46 mts.intechopen.com <1 %

Internet Source

---

47 Balvant Yadav, Anilkumar Gunnam, Rajesh Thipparaboina, Ashwini K. Nangia, Nalini R Shastri. "Hepatoprotective Cocrystals of Isoniazid: Synthesis, Solid State Characterization, and Hepatotoxicity Studies", Crystal Growth & Design, 2019 <1 %

Publication

---

48 Haobin Zhang, Changyan Guo, Xiaochuan Wang, Jinjiang Xu, Xuan He, Yu Liu, Xiaofeng Liu, Hui Huang, Jie Sun. "Five Energetic <1 %

# Cocrystals of BTF by Intermolecular Hydrogen Bond and $\pi$ -Stacking Interactions", Crystal Growth & Design, 2013

Publication

---

49

Nicholas D.K. Petraco. "Amino Acid Alanine Reactivity with the Fingerprint Reagent Ninhydrin. A Detailed Ab Initio Computational Study", Journal of Forensic Sciences, 11/2006

Publication

---

<1%

50

Ritu Rathi, Sukhanpreet Kaur, Inderbir Singh. "A Review on Co-crystals of Herbal Bioactives for Solubility Enhancement: Preparation Methods and Characterization Techniques", Crystal Growth & Design, 2022

Publication

---

<1%

---

Exclude quotes    On

Exclude matches    Off

Exclude bibliography    On

# Synthesis, Characterization and Dissolution Performance of Cocrystal of Cinnamic Acid with Nicotinamide: Experimental and Computation Investigation

---

GRADEMARK REPORT

---

FINAL GRADE

GENERAL COMMENTS

**/100**

---

PAGE 1

---

PAGE 2

---

PAGE 3

---

PAGE 4

---

PAGE 5

---

PAGE 6

---

PAGE 7

---

PAGE 8

---

PAGE 9

---

PAGE 10

---